2022 19th International Conference on Electrical Engineering, Computing Science and Automatic Control (CCE). Mexico City, Mexico. November 9-11, 2022

Automatic Delineation Algorithms of ECG Atrial Electrical Activity Waves Based on the Continuous Wavelet Transform with Splines

Dalila Rivera-Córdova
Bioelectronics Section, Electrical Engineering Department
CINVESTAV
Mexico City, Mexico
dalila.riverac@cinvestav.mx

Frank Martínez-Suárez
Bioelectronics Section, Electrical Engineering Department
CINVESTAV
Mexico City, Mexico
frank.martinez@cinvestav.mx

José Alberto García-Limón
Bioelectronics Section, Electrical Engineering Department
CINVESTAV
Mexico City, Mexico
josea.garcial@cinvestav.mx

Carlos Alvarado-Serrano
Bioelectronics Section, Electrical Engineering Department
CINVESTAV
Mexico City, Mexico
calvarad@cinvestav.mx

***Abstract*—This work presents algorithms based in the continuous wavelet transform with splines for the automatic delineation of the characteristic points of the P, Q and R waves. For the validation of the P wave start and end algorithm, 80 records from the QT database (QTDB) were used with manual annotations realized by experts, which were compared with the detections of the developed algorithms. The obtained errors were: 7.51 ± 7.23 ms for the start of P wave and 7.29 ± 5.86 ms for the end of P wave, which are below of the tolerance limits for deviations determined by the experts. The P and R waves peaks detection algorithms were evaluated with 18 and 11 records from QTDB respectively, and a sensitivity and positive predictivity over 99.5% were obtained.**

Keywords—ECG, delineation algorithms, P wave, R wave, wavelet transform, splines.

I. INTRODUCTION

The use and development of automatic algorithms for the delineation of characteristic points of ECG waves contribute to the diagnosis and treatment of many heart diseases, which are the main cause of death in the world [1]. Some abnormal characteristics of the P wave and PR interval corresponding to ECG atrial electrical activity have been associated with the atrial fibrillation [2]; therefore the automatic delineation of P and R waves onsets, peaks and ends for their measurement is important mainly for the monitoring and analysis of long-term recordings.

Several algorithms for the delineation of the P wave characteristic points have been proposed. There are methods based on the Fourier based filtering [3], low-pass differentiation [4], dynamic time warping [5], wavelet transform (WT) [6,7], WT with evolutionary algorithm [8], support vector machine (SVM) [9], phasor transform [10], Bayesian Approach and a Partially Collapsed Gibbs Sampler (PCGS) [11], discrete wavelet transform (DWT) with correlation analysis of templates [12] and phase free stationary WT [13].

With respect to the WT, it provides a description of the temporal characteristics of the signal at different scales or frequency bands; therefore, it reduces the influence of noise, artifacts and baseline drift in the signal using the appropriate scale [6,7].

In this work, the aim is to develop automatic algorithms for the P, Q and R waves delineation that represent the ECG atrial electrical activity, based on the continuous wavelet transform (CWT) with splines. Some of the evaluation results obtained in the QRS complex detection using a first version of these algorithms were presented in [14].

II. MATERIALS AND METHODS

A. Wavelet Transform

The continuous wavelet transform (CWT) is defined as the convolution of a time-continuous signal *x(t)* with a wavelet function $\psi(t)$ time shifted by a translation parameter b and dilated by a scale parameter a.

$$CWTx(a,b)\frac{1}{\sqrt{a}}\int_{-\infty}^{\infty}X(t)\psi^{*}=\left(\frac{t-b}{a}\right)dt \qquad (1)$$

B. Splines Functions

To evaluate the CWT at any integer scale we use splines which are quite flexible functions that allow to approximate virtually any desirable wavelet shape. *B*-splines are functions constructed from polynomial segments of degree *n* and unit length connected in a way to ensure the continuity of the resulting function and its derivatives up to order (*n*–1). These functions are similar to a Gaussian of compact support and are generated from the iterative convolution of a *B*-spline of degree zero that is the centered unit rectangular pulse [15].

In this method, the input signal $x(t)$ and the wavelet $\psi(t)$ are both represented by polynomial splines of degree n_1 and n_2 respectively and the resulting CWT at scale m is a polynomial spline function, then considering the values of the *B*-spline basis functions at the integers [15]:

$$CWT(x(t),m,k)=\sum_{k\in Z}\left([p]\uparrow_{m} * u_{m}^{n_2} * b^{n_1+n_2+1} * c\right)(k) \quad (2)$$

Where $[p]\uparrow_m(k)$ is the upsampling of the *B*-spline of the sequence *p* by a factor of *m*, $u_m^{n_2}$ is a cascade of (n_2 – 1) moving average filters of order (*m*–1) with a offset k_0 that ensures its symmetry, $b^{n_1+n_2+1}$ is the representation of a spline of order (n_1 + n_2 + 1) and *c*(*k*)'s are the *B*–spline coefficients.

This work has been funded by a scholarship from the CONACYT (México) to Dalila Rivera-Córdova.

978-1-6654-5508-4/22/$31.00 ©2022 IEEE

The wavelet function used $\psi(t)$ is the first derivate of a *B*–spline of 4th order expanded by a factor of two. This wavelet is well localized in both time and frequency because is similar to the first derivate of a Gaussian function (Fig. 2(a) in [15]).

C. Scale

The scale selection for the detection of the characteristic points of the P-wave plays an important role, since its selection will produce a dilation or compression of the function wavelet $\psi(t)$ so the CWT can extract the high and low frequency components of the signal $x(t)$. Fig. 1 shows the frequency response of the scales used by the algorithm at a sampling frequency of 250 Hz. Table 1 shows the scales with their respective bandwidths at - 3 dB of the equivalent digital filters for a sampling frequency (fs) of 250 Hz.

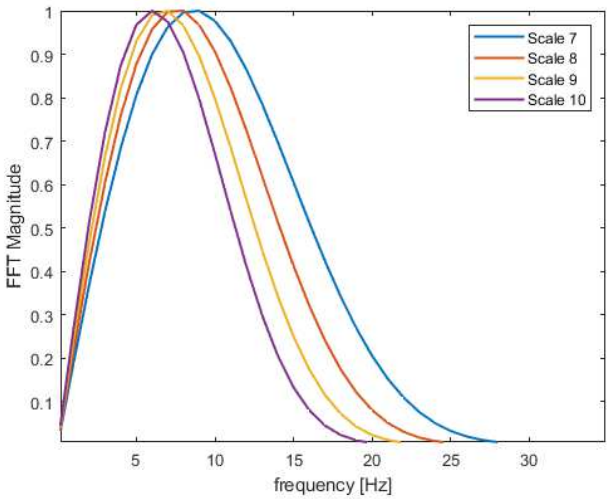

Fig. 1. Equivalent filter bandwidths at a sampling frequency, fs = 250 Hz.

TABLE 1. BANDWIDTHS AT -3 DB OF THE EQUIVALENT DIGITAL FILTERS.

Scale	Sampling Frequency =250 Hz
	Bandwidth (Hz)
1	28- 94
3	10- 32
7	4- 14
8	4- 12
9	3- 11
10	3- 10

D. Algorithm Development

1) R-wave peak detection

The R wave peak detection is fundamental for detection algorithms since, being the one with the highest amplitude in the ECG, it is used as a reference to detect other waves and intervals. The wavelet function used to detect R generates a pair of maximum values (Pmm) of opposite signs (Wmax and Wmin), where the zero crossing between them corresponds to the R peak The QRS complex comprises a frequency range from 3 Hz to 40 Hz, considering fs = 250 Hz is used scale 3. To consider that increasing the scale will also increase the delay. The algorithm developed by Alvarado et al. [14] was implemented with some modifications to detect other QRS complex types as qrS, rS or QS where the S wave of negative polarity is detected because it is larger in amplitude than the R wave of positive polarity. In this case, in the Pmm generated, Wmax is present first and after Wmin. For QRS complex types as qR, QRs, qRs, qRS and Rs, where the R wave is detected, in the Pmm, Wmin is present first and after Wmax (Fig. 2) [16,17].

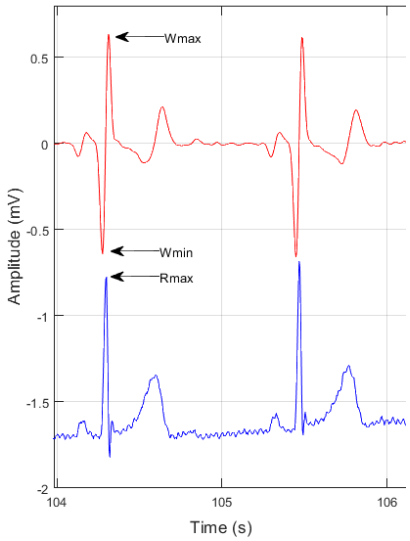

Fig. 2. ECG (bottom) and its CWT at scale 3 (top) for R-peak detection (Rmax).

The detection of the R wave peak (Rmax) starts by searching in the first 2 seconds for the first 2 Pmm (Wmax and Wmin) to define the thresholds (Umax and Umin). Then the first 2 Pmm above Umax and Umin are searched, as well as their zero crossings, these zero crossings correspond to the first two peaks of the R wave, then RR and RRav are defined, as well as HR. To find the following Rmax, a window of 200 ms is used at the beginning, which will be modified according to RRav (average RR), by this way if the Pmm found is greater than Umax and Umin, the RR and RRav values are recalculated and with them the thresholds. As a last step, a search for undetected Rmax is performed, using lower thresholds (Fig 3).

HR is a factor to consider in the development of the algorithm to detect the P wave, because it is different in each patient and can vary considerably in each recording, for this reason the search window is dependent on HR. Therefore, the window will have a smaller search range as the HR increases, and if the HR decreases the search range will be larger.

2) Q-wave onset and peak delineation

The delineation of the Q-wave peak is performed from a backward search window of the R-wave peak. The first step is to find the first zero-crossing (Qa) to the left of Wmin, then another backward search is performed to find the next zero crossing (Qi) (Fig. 4 a)). In the case of Q peak detection, scale 3 is used, the same as the one used in the R wave peak detection. The flowchart of the Q onset and peak delineation algorithm is shown in Fig. 5.

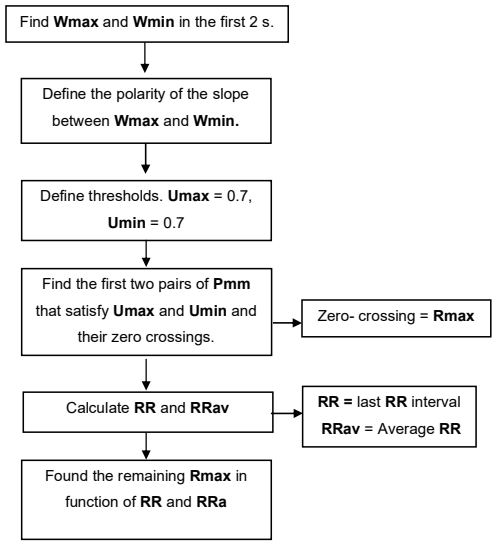

Fig. 3. Flowchart for R wave peak (Rmax) detection.

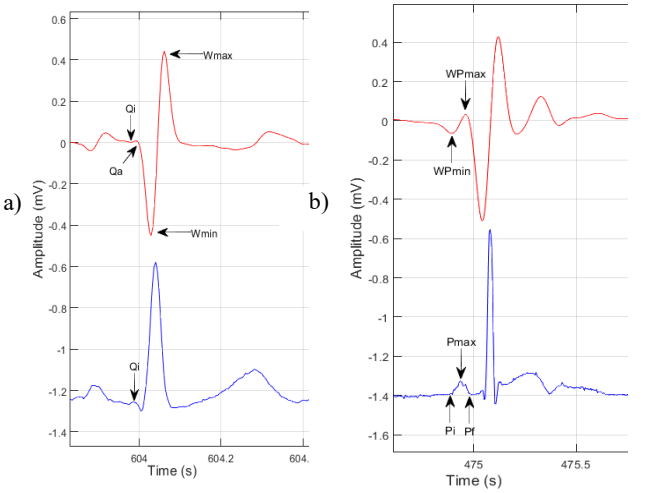

Fig. 4. a) ECG (bottom) and its CWT at scale 3 (top) for Q onset (Qi) and Q peak (Qa) delineation. b) ECG (bottom) and its CWT at scale 8 (top) for the P peak detection (Pmax)

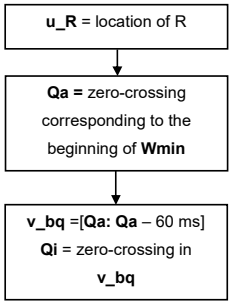

Fig. 5. Flowchart for Q onset (Qi) and Q peak (Qa) delineation.

3) P-wave onset, peak and end delineation

In P wave delineation, the location of the R wave peak is used, because from this location a backward search window is applied to calculate the beginning and end of the P wave. It is in these search windows that the wavelet function obtained from the ECG recording is analyzed. The zero crossing between the maximum moduli generated by the CWT (Pmm) corresponds to the P wave peak (Pmax). The beginning of the maximum value of negative sign (wPmin) indicates the P wave onset and the end of the maximum value of positive sign (wPmax) determines the P wave end.

Fig. 4 b) shows an ECG recording and the maximum and minimum values generated by the CWT at scale 8, as well as the zero crossing between these two. Due to the low amplitude and the frequency range of the P-wave it is convenient to use high scales, specifically this wave handles a frequency spectrum in the range of 0.5 Hz to 10 Hz, so it is decided to use scale 8 and 10, and for some cases scale 9. It is important to consider that the maximum peak of the P wave will have a delay depending on the scale that is decided to use.

In the P-wave delineation, the Pmax location obtained from the CWT signal is used to apply a backward search window. In this window, WPmax and WPmin are searched, where the zero crossing between these two corresponds to Pmax, then the thresholds (uP1 and uP2) are defined. To define the onset of the P wave (Pi) a backward search window is performed, from WPmin to the beginning of the window (vi) where the value is equal or greater than UP1 will indicate the onset of the P wave and for the end of the P wave (Pf) a search window is performed from WPax to the end of the window (vf), Pf will be where a value equal or greater than uP2 is found (Fig. 6).

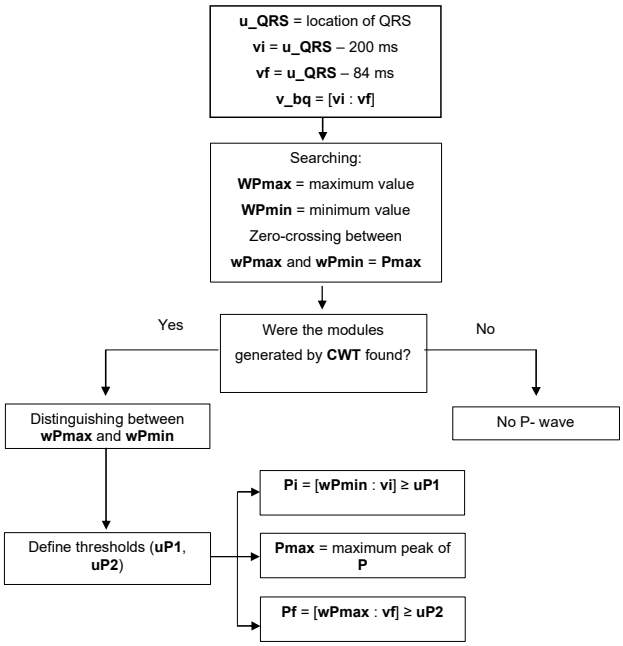

Fig. 6. Flowchart for P wave onset (Pi), P wave peak (Pmax) and P wave end (Pf) delineation.

III. Results and Discussion

The QT database was used to validate the algorithms for R wave peak detection and delineation of P wave onset, peak and end. This database consists of 105 recordings of 15 min each, obtained from a two-channel Holter. These recordings were chosen from the following databases: MIT- BIH Arrhythmia (MIT- BIH), European Society of Cardiology ST- T (ESC-STT) and from several databases collected at Boston's Beth Israel Deaconess Medical Center (BIDMC) [18].

A. R-wave peak detection

Fig. 7 shows the R wave peak detection in an ECG recording with qRs complex type, while Fig. 8 shows the detection of the S peak in a recording with rS complex type. (In both figures ECG top, CWT bottom)

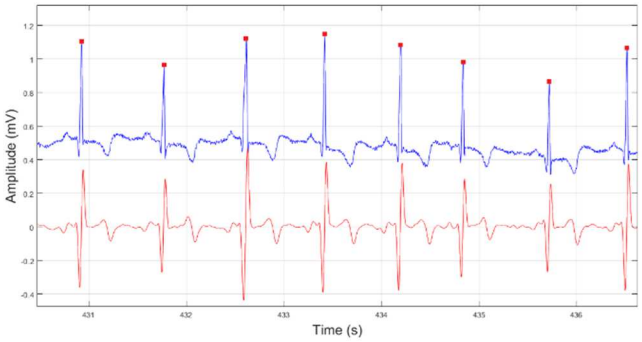

Fig. 7. ECG (top) with type of complex qRs from sel100 record and CWT (bottom) at scale 3.

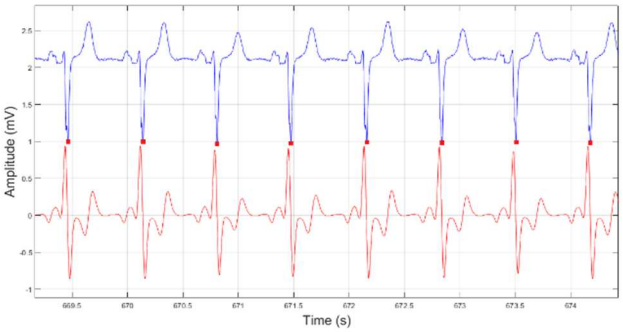

Fig. 8. ECG (top) with type of complex rS from sel302 record and CWT (bottom) at scale 3.

To evaluate the performance of the R-wave peak detection algorithm, 11 records from the QT database were used. Records with different electrocardiographic trace morphologies were selected to evaluate the performance of the algorithm under different conditions and thus validate its operation. The results obtained from the validation of the R-wave peak detection algorithm are shown in Table 2, the false positives and negatives obtained in each recording and the percentage of error are presented. The parameters used for the evaluation of the developed algorithms are the sensitivity *Se* (%) and the positive predictivity $P+$ (%) for the QRS complex detector:

$$Se = \frac{TP}{TP + FN} \tag{3}$$

$$P+ = \frac{TP}{TP + FP} \tag{4}$$

Where TP is the number of true positives, FN is the number of false negatives and FP is the number of false positives.
The performance of the algorithm for R-wave peak detection obtained a sensitivity of 99.56%, a positive predictivity of 99.91% and an error rate of 0.33%.

TABLE 2. Evaluation of the R-wave peak detection algorithm on 11 records from QT database.

Records	Total beats	Beats recorded	FP	FN	False detections	
					Beats	*% error*
Sel100	1134	30	0	0	0	0
Sel103	1048	30	0	0	0	0
Sel114	837	50	1	21	22	0.8
Sel117	766	30	2	1	3	0.07
Sel123	755	30	0	1	1	0.10
Sel302	1499	30	2	3	5	0.01
Sel803	1012	30	1	11	12	0.85
Sele0104	802	30	2	2	4	1.5
Sele0106	896	30	0	0	0	0
Sele0107	812	34	0	0	0	0
Sele0111	905	30	1	2	3	0.31
Totals	**10466**	**354**	**9**	**41**	**50**	**0.33**

B. P- wave onset, peak and end delineation

For the evaluation of the algorithm, only the records with manual annotations of the P-wave in the QT database were selected, evaluating 80 records in total. The results obtained by evaluating the detection algorithm are compared with the manual annotations made by experts. Although the algorithm is able to automatically identify P wave onset, peak and end, only the comparison with the values of the onset and end of this wave is performed, because there are only standards for the evaluation of these two points of the P wave known as Common Standards for Electrocardiography (CSE) [19]. To properly evaluate the performance of the algorithm, different ECG recordings were used, from those with supraventricular arrhythmias to recordings of patients with sudden death, in order to assess the performance of the algorithm under different ECG morphologies (Fig. 9).

To evaluate the performance of the P-wave peak detection algorithm, 18 records from the QT database were used. Table 3 shows the results obtained from the validation of this algorithm. The false positives and negatives of each record and their percentage error are shown. When evaluating the performance of the algorithm for P peak detection, a sensitivity of 99.61%, a positive predictivity of 99.83% and an error rate of 0.41% were obtained.

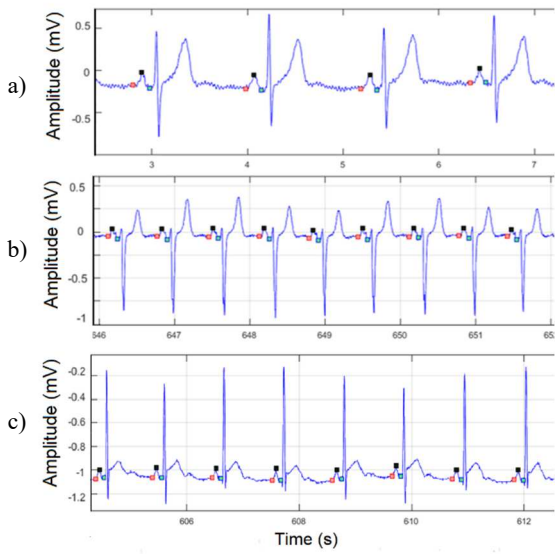

Fig.9. Segments of ECG recordings from the QT database with detections of the P-wave onset, peak and end. a). Record sel117. b). Record sel302. c). Record sel0104.

TABLE 3. EVALUATION OF THE P-PEAK DETECTION ALGORITHM ON 18 RECORDS FROM QT DATABASE.

Records	Total beats	Beats recorded	FP	FN	False detections	
					Beats	*% error*
Sel100	1134	30	3	4	7	0.09
Sel103	1048	30	0	1	1	0.10
Sel114	843	50	3	23	26	1.36
Sel116	1183	50	1	4	5	0.4
Sel117	766	30	3	4	7	0.06
Sel123	755	30	1	2	3	0.08
Sel213	1636	71	3	8	11	0.78
Sel233	1220	30	5	6	11	0.58
Sel301	1351	30	2	2	4	1.13
Sel302	1495	30	3	3	6	0.09
Sel306	1039	36	0	0	0	0
Sel307	857	30	0	0	0	0
Sele0104	802	30	1	2	3	0.66
Sele0106	896	30	0	1	1	1.54
Sele0107	812	34	2	1	3	0.08
Sele0110	872	30	1	0	1	0.42
Sele0112	683	50	2	4	6	0.07
Sele0411	1199	30	1	2	3	0.01
Totales	**18591**	**651**	**31**	**67**	**98**	**0.41**

For the validation of the delineation of P wave onset and end is calculated the standard deviation of the differences between expert manual annotations and automatic annotations performed by the algorithms [19]. Table 4 shows the total differences of manual expert and automatic algorithm annotations of the P wave onset and end of the databases that constitute the QT database. Table 5 shows the total average of the differences in all the evaluated records of the manual annotations and those performed by the algorithms, and the standard established by the CSE [19].

TABLE 4. TOTAL DIFFERENCES OF MANUAL EXPERT AND AUTOMATIC ALGORITHM ANNOTATIONS OF THE P WAVE ONSET (Pi) AND END (Pf)

Database	$m \pm sd$ (ms)	
	Pi	Pf
MIT-BIH Arrhythmia	8.07 ± 8.66	9.14 ± 8.86
MIT-BIH ST DB	7.43 ± 5.79	7.08 ± 6.54
MIT-BIH Sup. Vent	6.62 ± 4.71	6.56 ± 4.82
MIT-BIH Long term	9.14 ± 11.84	7.05 ± 2.80
ESC STT	7.23 ± 5.72	8.60 ± 6.95
MIT-BIH NSR DB	6.61 ± 7.61	7.18 ± 6.74
Sudden Death	7.50 ± 6.30	5.33 ± 4.35

TABLE 5. TOTAL AVERAGE OF DIFFERENCES OF MANUAL EXPERT ANNOTATIONS AND AUTOMATIC ALGORITHM ANNOTATIONS OF THE P WAVE ONSET (Pi) AND END (Pf).

Total number of beats recorded	P- wave onset and end	$m \pm sd$ (ms)	Tolerance limits for standard deviation accepted by CSE (ms)
2683	Pi	7.51 ± 7.23	10.2
	Pf	7.29 ± 5.86	12.7

Table 6 compares some works of detection and delineation of the P wave characteristic points with the developed algorithms. For recordings of the QTDB, the P wave peak sensitivity is higher than that obtained by J.P. Martínez et al. [6], R.N. Costandy et al. [21] and L. Saclova et al. [22], and lower than L. Marsanova et al. [20]. P wave peak positive predictivity is also higher than that obtained by J.P. Martínez et al. [6], R. N. Costandy et al. [21] and L, Saclova et al. [22], and similar to that of L. Marsanorva et al. [20].

TABLE 6. DELINEATION AND DETECTION COMPARISON OF P WAVE CHARACTERISTIC POINTS.

Database	Author	P_{peak}		P_i	P_f
		Se (%)	P^+ (%)	$m \pm sd$	
QTDB	This work	99.61	99.83	7.51±7.23	7.29±5.86
QTDB	J.P. Martínez et al. [6]	98.87	91.03	2.0 ±14.8	1.9 ± 12.8
QTDB	G. Lenis et al. [13]	N/R	N/R	-0.3±12.4	N/R
QTDB	L. Marsanova et al. [20]	99.84	99.84	N/R	N/R
QTDB	R.N. Costandy et al. [21]	97.24	97.22	N/R	N/R
QTDB	L. Saclova et al. [22]	99.23	99.12	N/R	N/R

For validation of the P-wave onset and end delineation algorithms, 80 records from the QT database were used with manual annotations performed by CSE experts [19]. Table 5 shows that for the P-wave onset and end, errors of 7.51 ± 7.23 ms and 7.29 ± 5.86 ms are obtained, respectively, which are within the tolerance limits for deviations from CSE experts [19]. In both cases the values of the standard deviation are inferior to those obtained by J.P. Martínez et al. [6], and for P wave onset is lower than the obtained by G. Lenis et al. [13]. Note that the sampling period in the QT database is 4 ms.

IV. Conclusions

In this work, we have presented automatic algorithms for the delineation of characteristic points of P, Q and R waves based on the CWT with splines. This method allows to use a wide range of scales and to reduce the influence of noise, artifacts and baseline drift in the ECG signal. The developed algorithms have been validated with ECG recordings from the QT database representing a total of 354 beats for QRS detection, 651 beats for P-wave peak detection and 2,683 beats for P-wave onset and end delineation. The results obtained are comparable with those of other published algorithms. The algorithms can detect R-wave and P-wave peaks with high sensitivity. The errors in the delineation of the P-wave onset and end are within the tolerance limits for deviations from manual measurement by CSE experts. These algorithms allow the measurement and analysis of ECG atrial electrical activity represented by the P wave and PR interval mainly in long-term recordings clinically useful for cardiac diagnostic and prognostic.

References

[1] World Health Organization (WHO). Cardiovascular Diseases (CVDs) [Internet]. 2021-06-11. Available from: https://www.who.int/news-room/fact-sheets/detail/cardiovascular-diseases-(cvds) [Accessed: June 20, 2022].

[2] D.M. German, M.M. Kabir, T.A. Dewland, C.A. Henrikson, L.G. Tereshchenko, "Atrial Fibrillation Predictors: Importance of the Electrocardiogram," *Ann Noninvasive Electrocardiol*, vol. 21 no. 1, pp. 20–29, 2016, doi: 10.1111/anec.12321.

[3] I.S.N. Murthy, U.C. Niranjan, "Component wave delineation of ECG by filtering in the Fourier domain," *Med Biol Eng Comput.*, vol. 30, no. 2, pp. 169–176, 1992, doi: 10.1007/BF02446127.

[4] P. Laguna, R. Jané, and P. Caminal, "Automatic detection of wave boundaries in multilead ECG signals: Validation with the CSE database," *Comput. Biomed. Res.*, vol. 27, no. 1, pp. 45–60, 1994, doi: 10.1006/cbmr.1994.1006.

[5] H. J. L. M. Vullings, M. H. G. Verhaegen and H. B. Verbruggen, "Automated ECG segmentation with dynamic time warping," in *Proceedings of the 20th Annual International Conference of the IEEE Engineering in Medicine and Biology Society. Vol. 20 Biomedical Engineering Towards the Year 2000 and Beyond*, 1998, pp. 163–166 vol.1, doi: 10.1109/IEMBS.1998.745863.

[6] J. P. Martinez, R. Almeida, S. Olmos, A. P. Rocha and P. Laguna, "A wavelet-based ECG delineator: evaluation on standard databases," *IEEE Trans Biomed Eng.*, vol. 51, no. 4, pp. 570–581, 2004, doi: 10.1109/TBME.2003.821031.

[7] A. Ghaffari, M.R. Homaeinezhad, M. Akraminia, M. Atarod, M. Daevaeiha, "A robust wavelet-based multi-lead electrocardiogram delineation algorithm," *Med Eng Phys*., vol. 31, no. 10, pp. 1219–1227, 2009, doi: 10.1016/j.medengphy.2009.07.017.

[8] J. Dumont, A. I. Hernandez and G. Carrault, "Parameter optimization of a wavelet-based electrocardiogram delineator with an evolutionary algorithm," in *Computers in Cardiology 2005,* 2005, pp. 707–710, doi: 10.1109/CIC.2005.1588202.

[9] S.S. Mehta, N.S. Lingayat, "Development of SVM based classification techniques for the delineation of wave components in 12-lead electrocardiogram," *Biomed Signal Process Control*, vol. 3, no. 4, pp. 341–349, 2008, https://doi.org/10.1016/j.bspc.2008.04.002.

[10] A. Martínez, R. Alcaraz and J. J. Rieta, "Automatic electrocardiogram delineator based on the Phasor Transform of single lead recordings," in *2010 Computing in Cardiology*, 2010, pp. 987–990.

[11] C. Lin, C. Mailhes and J.I. Tourneret, "P- and T-Wave delineation in ECG signals using a Bayesian approach and a partially collapsed Gibbs sampler," *IEEE Trans. Biomed. Eng.*, vol. 57, no. 12, pp. 2840–2849, 2010, doi: 10.1109/TBME.2010.2076809.

[12] A. Karimipour, M.R. Homaeinezhad, "Real-time electrocardiogram P-QRS-T detection-delineation algorithm based on quality-supported analysis of characteristic templates," *Comput. Biol. Med*., vol. 52, pp. 153–165, 2014, doi: 10.1016/j.compbiomed.2014.07.002.

[13] G. Lenis, N. Pilia, T. Oesterlein, A. Luik, C. Schmitt, O. Dössel, "P wave detection and delineation in the ECG based on the phase free stationary wavelet transform and using intracardiac atrial electrograms as reference," *Biomed. Eng.-Biomed. Tech.,* vol. 61, no. 1, pp. 37–56, 2016, doi: 10.1515/bmt-2014-0161.

[14] C. Alvarado, J. Arregui, J. Ramos and R. Pallas-Areny, "Automatic detection of ECG ventricular activity waves using continuous spline wavelet transform," in *2005 2nd International Conference on Electrical and Electronics Engineering*, 2005, pp. 189-192, doi: 10.1109/ICEEE.2005.1529605.

[15] M. Unser, A. Aldroubi and S. J. Schiff, "Fast implementation of the continuous wavelet transform with integer scales," *IEEE Transactions on Signal Processing*, vol. 42, no. 12, pp. 3519-3523, 1994, doi: 10.1109/78.340787.

[16] M. L. Corzo-Cuesta and C. Alvarado-Serrano, "An Algorithm for QT Dispersion Analysis: Validation and Application in Chronic Kidney Disease," in *2016 13th International Conference on Electrical Engineering, Computing Science and Automatic Control (CCE)*, 2016, pp. 1-6, doi: 10.1109/ICEEE.2016.7751237.

[17] M. Baltazar Leal, "Método de estimación del final de la onda T del ECG durante ejercicio intenso para el análisis de la dinámica del intervalo RT en pruebas de ejercicio", Tesis de Maestría, Sección de Bioelectrónica, Departamento de Ingeniería Eléctrica, Cinvestav, Ciudad México, México, 2015.

[18] P. Laguna, R.G. Mark, A. Goldberg, and G.B. Moody, "A database for evaluation of algorithms for measurement of QT and other wave form intervals in the ECG," in *Computers in Cardiology 1997*, 1997, pp. 673-676, doi: 10.1109/CIC.1997.648140.

[19] The CSE Working Party, "Recommendations for measurement standards in quantitative electrocardiography," *Eur. Heart J*., vol. 6, no. 10, pp. 815–825, 1985, https://doi.org/10.1093/oxfordjournals.eurheartj.a061766

[20] L. Marsanova, A. Nemcová, R. Smísek, M. Vítek, et al., "Advanced P Wave Detection in ECG signals During Pathology: Evaluation in Different Arrhythmia Contexts," *Sci. Rep.*, 9, 19053, 2019, https://doi.org/10.1038/s41598-019-55323-3.

[21] R.N. Costandy, S.M. Gasser, M.S. El-Mahallawy, M.W. Fakhr, S.Y. Marzouk, "P-Wave Detection Using a Fully Convolutional Neural Network in Electrocardiogram Images," *Appl. Sci.*, vol. 10, no. 3, 976, 2020, https://doi.org/10.3390/app10030976.

[22] L. Saclova, A. Nemcova, R. Smisek, L. Smital, et al., "Reliable P wave detection in pathological ECG signals," *Sci. Rep.* 12, 6589, 2022. https://doi.org/10.1038/s41598-022-10656-4.